Electronic Supplementary Material (ESI) for New Journal of Chemistry.

Electronic Supplementary Information for

Preparation of $Bi_3Fe_{0.5}Nb_{1.5}O_9$/g-C_3N_4 heterojunction photocatalyst and application in photocatalytic degradation of 2,4-dichlorophenol in environment

Jingdao Wang, Yuanling Sun, Hao Liu, Yanan Hou, Yuxue Dai, Chuannan Luo*, Xueying Wang *

Key Laboratory of Interfacial Reaction & Sensing Analysis in Universities of Shandong, School of Chemistry and Chemical Engineering, University of Jinan, Jinan 250022, PR China

*Corresponding author: Tel.: +86 0531 89736065. Dr. Xueying Wang and Pro. Chuannan Luo are both the corresponding author of this article.

E-mail address: chm_wangxy@ujn.edu.cn (Xueying Wang); chm_yfl518@163.com (Chuannan Luo)

2.1 Materials and apparatus

Materials

All reagents were analytical grade and used without further processing. Melamine (99%), ammonium chloride (NH_4Cl; AR, 99.5%), potassium chloride (KCl; AR, 99.5%), bismuth nitrate pentahydrate ($Bi(NO_3)_3·5H_2O$; AR, 99.0%), ferric Nitrate Nonahydrate ($Fe(NO_3)_3·9H_2O$; AR, 98.5%), niobium pentaoxide (Nb_2O_5; AR, 99.9%), barium sulfate ($BaSO_4$; SP), sodium sulfate (Na_2SO_4; AR, 99%), isopropyl alcohol (C_3H_8O; AR, 99.5%), triethanolamine ($C_6H_{15}NO_3$; AR, 98%), benzoquinone ($C_6H_4O_2$; 97%), and ethylene glycol monomethyl ether (AR) were purchased from Macklin. Absolute ethanol (99.5%), sodium hydroxide (NaOH; AR), and ammonia

($NH_3 \cdot H_2O$; AR) were obtained from Sinopharm Chemical Reagent Co., Ltd.

Apparatus

The Zeta potential is measured on Zetasizer Nano-ZS 90 (Malvern Instruments). The crystallinity and phase structure of the samples were analyzed by X-ray diffractometer (XRD; Bruker, German) under Cu *Kα* radiation. The geometric morphology and size of the samples were observed by scanning electron microscope (SEM), and energy dispersive X-ray spectroscopy (EDS) was carried out on the Hitachi SX-650 machine (Tokyo, Japan). The images of transmission electron microscope (TEM) and high resolution transmission electron microscope (HRTEM) were collected on JEM 2010 machine (Tokyo, Japan), and the geometric morphology and size of the samples were further observed. The specific surface area and pore structure of the materials were obtained by N_2 adsorption-desorption by KuboX1000 and Brunauer-Emmett-Teller (BET) method. The surface chemical state and chemical composition of the samples were analyzed by X-ray photoelectron spectroscopy (XPS, ThermoESCALAB 250 XI) and C1s peak (284.4 eV) as a reference. The UV-visible diffuse reflectance spectrum (DRS) was collected by UV-3600 ultraviolet-visible spectrophotometer to reflect the optical absorption properties and optical absorption range of the sample, and the energy band gap of the sample was calculated by subsequent formula conversion. The photoluminescence spectrum (PL, FLS 920) was detected by light with incident wavelength of 310 nm and excitation wavelength of 434 nm. Under the condition of dark and visible light irradiation, the electron spin resonance (ESR) signals of superoxide radical ($\cdot O_2^-$) and hydroxyl radical (OH) were

identified by Brukera 300 spectrometer.

2.2.1 Preparation of graphite-phase carbon nitride nanosheets (g-C_3N_4)

g-C_3N_4 are prepared by thermal Polycondensation of cheap nitrogen-rich precursors such as dicyandiamide, cyanamide, melamine or urea, and then thermal etching in air. The mixture was transferred to a porcelain crucible and heated to 550°C at a heating rate of 5°C/min in a muffle furnace and kept for 4 h. After cooling to room temperature, the samples were ground and washed with deionized water and ethanol for several times, and then dried in a vacuum drying box at 60°C for 12 h. Finally, the obtained powder was placed in an open porcelain crucible and heated to 500°C at a heating rate of 10°C/min and kept for 2 hours. After cooling to room temperature, the yellow powder was fully ground to obtain the product.

The synthesis process of g-C_3N_4 was very mature, and the surface alkalization was also a proven mature method. Therefore, g-C_3N_4 was not discussed as the main content in the text. Three carbon nitrides were prepared by combining references and objective experimental conditions with potassium chloride, melamine and ammonium chloride at mass ratios of 7.5, 1.5 and X (X = 0.1, 0.2 and 0.3), respectively. Which were recorded as CNK/0.1 NH_4Cl, CNK/0.3 NH_4Cl, CNK/0.5 NH_4Cl. As shown in Figure S4, It was clear that CNK/0.1 NH_4Cl showed an ideal stacked lamellar structure. The surface alkalinization of g-C_3N_4 was promoted by the introduction of KCl and NH_4Cl in situ synthesis. K ions played an important role in breaking the periodic chemical structure of g-C_3N_4, while the trace amount of H_2O in melamine could provide OH ions to graft hydroxyl groups. Surface hydroxyl groups can effectively trap holes to reduce recombination of light-generated carriers. The NH_4Cl mainly contributed to exfoliation of layered g-C_3N_4 particles and pushing negative shift of the conduction-band level. This suggests that surface/interface engineering of semiconductor photocatalysts is an effective way to improve photocatalytic efficiency [1-4].

2.3.1 Photocatalytic degradation of 2,4-Dichlorophenol

2,4-dichlorophenol (2,4-DCP) was selected as the target pollutant. The photocatalytic activity of the prepared materials was evaluated under visible light irradiation. Visible light was obtained by a 300 W xenon lamp (PLS-SXE 300 C). The experiment of photocatalytic degradation was carried out in the photoreaction protection box (LIGHTCUBE 2.3). The specific process is as follows: 300 mg of photocatalyst was dispersed into 200 mL 2,4-DCP solution (100 mg/L). The suspension was stirred magnetically for 60 min under light-proof conditions before light illumination to establish the adsorption-desorption equilibrium. Then, the light source was turned on and 10 mL of supernatant was collected regularly. The concentration changes before and after degradation of 2,4-DCP were analyzed by UV-2550 spectrophotometer. The total organic carbon (TOC) was measured by TOC analyzer (Shimadzu).

Free radical capture experiments were carried out to illustrate the contribution of main active species to the photocatalytic degradation of 2,4-DCP. Among them, benzoquinone (BQ), triethanolamine (TEOA) and isopropanol (IPA) were used as scavengers of superoxide radical ($\cdot O_2^-$), hole (h^+) and hydroxyl radical ($\cdot OH$), respectively. The trapping agent was introduced into the catalyst-2,4-DCP system prior to the photocatalytic degradation experiments, and the photocatalytic degradation experiments were carried out under the same conditions. A comparison with the blank experiment was performed to determine which active substance played

a role in the reaction process.

2.3.2 Electrochemical performance test of catalyst.

The photocurrent response, electrochemical impedance spectroscopy (EIS) and Mott-Schottky curves of the samples were measured on the electrochemical workstation (RST 5200 F) using the standard three-electrode method. The photocurrent response was measured using ITO/catalyst electrode as working electrode, while EIS and Mott-Schottky curves were measured using glassy carbon electrode/catalyst as working electrode. Pt electrode and Ag/AgCl electrode are used as counter electrode and reference electrode respectively, and the electrolyte is 0.1 M Na_2SO_4 solution. Using EIS-300 software, the Mott-Schottky curve is obtained in the potential range of -1.5 V-1.5 V (potential scale: 10 mV) at the frequency of 2.0 and 3.0 kHz, respectively. The frequency range of EIS is 0.1-10000 Hz, the amplitude is 5 mV, and the initial voltage is 0 V.

3.3. Photocatalytic activity

The photocatalytic performance of BFNO/CN was evaluated by catalyzing the degradation of target pollutant 2,4-DCP under visible light. A physical blend of the same mass ratio, named BFNO/CN-66P, was also prepared on the basis of BFNO/CN-66. Which was homogeneously mixed by means of a vortex mixer and then subjected to control experiments. Prior to illumination, the catalyst and 2,4-DCP solutions were mixed and placed in the dark and stirred to ensure that the adsorption-desorption equilibrium was achieved. Subsequently, a small amount of supernatant was periodically taken under visible light irradiation to analyze the change of 2,4-DCP concentration. Blank experiment showed that the self-degradation rate of 2,4-DCP under visible light was negligible.

Photodegradation of 2,4-DCP by BFNO/CN-66 under different reaction conditions

In order to explore the potential of BFNO/CN-66 in practical application, different water substrates were selected and the degradation experiments were carried out under visible light irradiation. The experimental steps of degradation are the same as the previous steps, except that the target pollutant 2,4-DCP is dissolved in different water substrates. In the experiment, ultra-pure water was used as the water substrate, and the degradation of 2,4-DCP under visible light was taken as the control group. The other water substrates selected were tap water, which was taken from the faucet in the laboratory, and artificial lake water, which was taken from the artificial lake water sample of the school, and the sampling time was May. Before the degradation experiment, these two kinds of solid water substrates are filtered through a 0.45 μm filter membrane. After that, a 25mg/L solution with the concentration of 2,4-DCP was prepared, which was used in the photodegradation experiment. The experimental results are shown in Fig. S3 and Table S4. The degradation effect of 2,4-DCP in tap water (78.6%) is similar to that in ultra-pure water (83.7%), but the degradation effect in lake water (51.8%) is lower than that in ultra-pure water. This may be due to the existence of some organic matter, impurities or salt ions in the lake water, which will occupy the active sites on the surface of BFNO/CN-66, thus inhibiting the degradation of 2,4-DCP. Then, the ultra-pure water was selected as the water substrate, and the solution with the concentration of 25mg/L was prepared and

irradiated directly in the sun to carry out the photodegradation experiment, and the rest of the experimental steps remained unchanged. The time of the experiment is noon in November in Jinan, and the outdoor temperature is about 25℃. Meanwhile, from the degradation curve (Fig. S3), ultra-pure water was selected as the aqueous substrate and the degradation of 2,4-DCP under sunlight was not as effective as the control group. It is probably that the intensity of sunlight is weaker than that of visible light (300 W), and there are still some uncontrollable factors in the environment. Generally speaking, BFNO/CN-66 still has good practical application potential.

Table S1

Degradation effect and reaction rate k value of photocatalytic degradation of 2,4-DCP in different reaction systems 90min

Materials	C_t/C_0	K(min^{-1})	Degradation rate (%)
g-C_3N_4	0.883	0.0008	11.7
BFNO/CN-33	0.455	0.0058	54.5
BFNO/CN-50	0.305	0.0086	69.5
BFNO/CN-66	0.163	0.0137	83.7
BFNO	0.789	0.0016	21.1

Table S2

Removal rate of TOC in different reaction systems

Materials	g-C_3N_4	BFNO/CN-33	BFNO/CN-50	BFNO/CN-66	BFNO
Removal rate of TOC (%)	13.2	49.9	58.1	64.2	17.2

Table S3

Degradation effect of five BFNO/CN-66 cycle experiments

Times	1	2	3	4	5
C_t/C_0	0.163	0.192	0.241	0.275	0.319
Degradation rate (%)	83.7	80.8	75.9	72.5	68.1

Table S4

Photodegradation of 2,4-DCP by BFNO/CN-66 under different reaction conditions

Conditions visible light	C_t/C_0	Degradation rate (%)
Ultra-pure water (Visible light)	0.163	83.7
Tap water (Visible light)	0.214	78.6
lake water (Visible light)	0.482	51.8
Ultra-pure water (Sunlight)	0.621	37.9

Table S5

Degradation effect after adding different trapping agents

Trapping agent	None	Benzoquinone	Triethanolamine	Isopropyl alcohol
C_t/C_0	0.163	0.564	0.489	0.342

Table S6

S. No	Name of the material	Degradation time (min)	Degradation rate (%)	References
1	$Bi_3Fe_{0.5}Nb_{1.5}O_9$/g-C_3N_4	120	83.7	This study
2	CeO_2/g-C_3N_4/NH_2-MIL-101(Fe)	120	87	[5]
3	5Zn/7Bi-PLFO	120	77	[6]
4	C/Bi/Bi_2O_3	300	65	[7]
5	Pd/Ni-WO_3/Mo: $BiVO_4$	240	45	[8]
6	$ZnNb_2O_6$/g-C_3N_4	180	95	[9]
7	CuS@CNs	240	94.9	[10]
8	$Na_{(8)}B_{(6)}$–CN	240	90.6	[11]

Figure S1

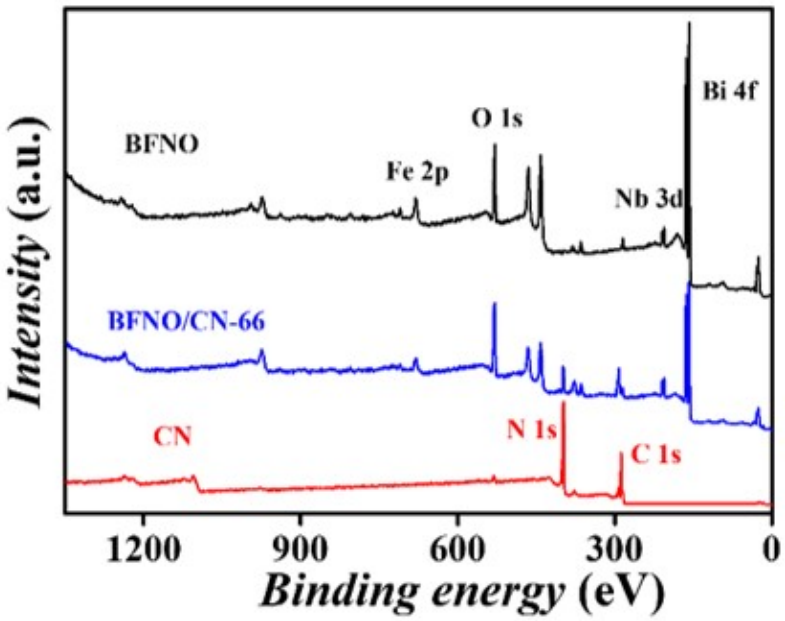

Figure S1 XPS spectra of BFNO, BFNO/CN-66 and g-C_3N_4

Figure S2

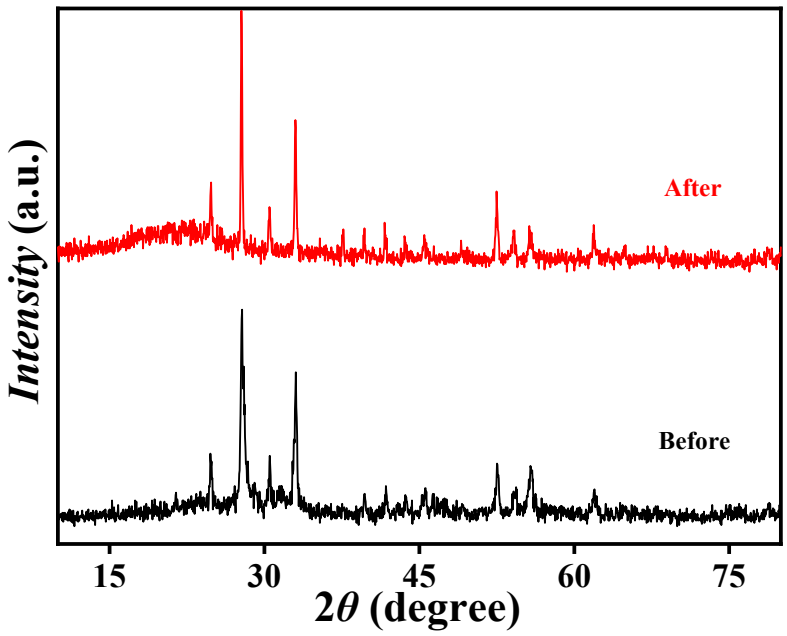

Figure S2 XRD patterns of 2,4-DCP before and after photocatalytic reaction

Figure S3

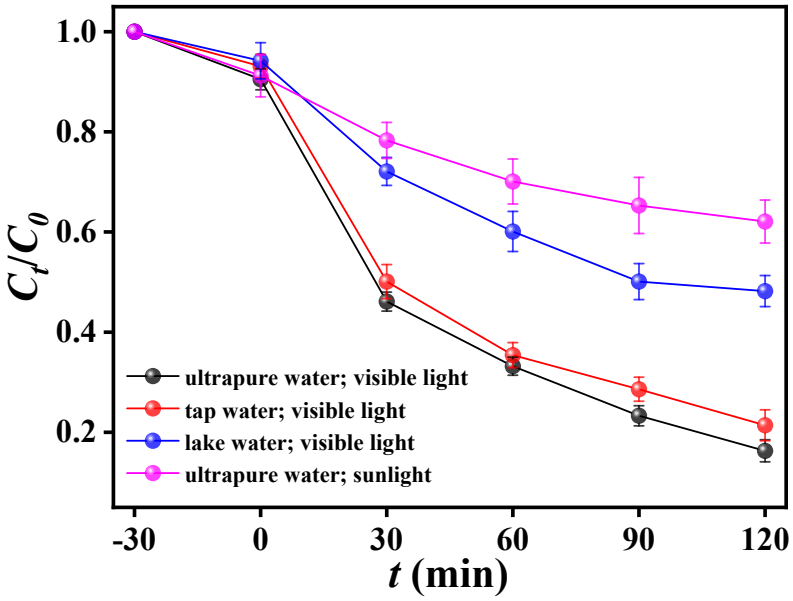

Figure S3 Photodegradation curves of 2,4-DCP by BFNO/CN-66 under different reaction conditions

Figure S4

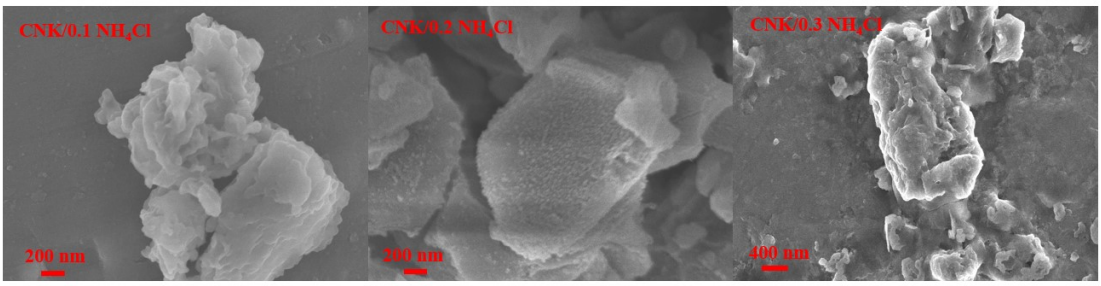

Figure S4 SEM images of CNK/0.1 NH_4Cl, CNK/0.3 NH_4Cl, CNK/0.5 NH_4Cl

Figure S5

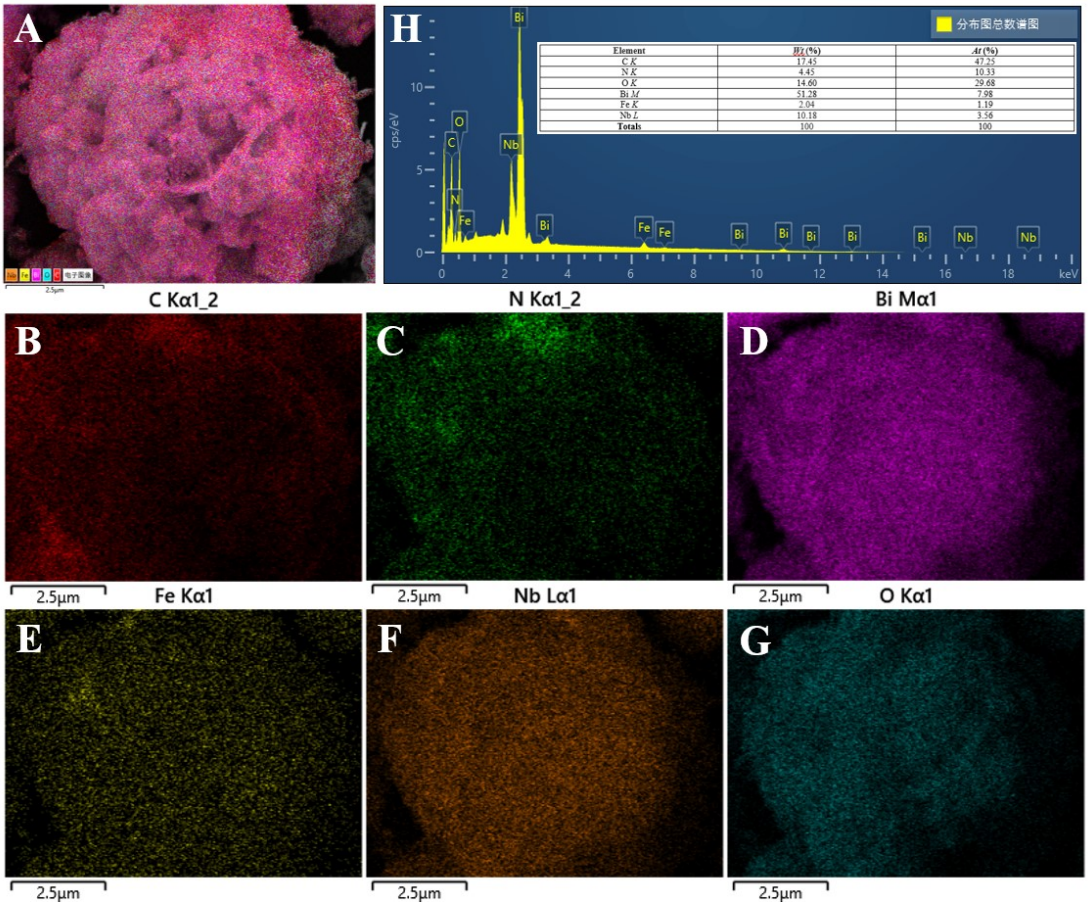

Figure S5 EDS mapping of BFNO/CN-66 (A), mapping of C (B), N (C), Bi (D), Fe (E), Nb (F), O (G), EDS spectra of BFNO/CN-66 (H).

References:

[1] Y. Li, H. Xu, S. Ouyang, D. Lu, X. Wang, D. Wang, J. Ye, In situ surface alkalinized g-C_3N_4 toward enhancement of photocatalytic H_2 evolution under visible-light irradiation, J. MATER CHEM A, 4(2016) 2943-2950.

[2] T. Xiong, W. Cen, Y. Zhang, F. Dong, Bridging the g-C_3N_4 Interlayers for Enhanced Photocatalysis, ACS CATAL, 6(2016) 2462-2472.

[3] W. Wang, H. Zhang, S. Zhang, Y. Liu, G. Wang, C. Sun, H. Zhao, Potassium-Ion-Assisted Regeneration of Active Cyano Groups in Carbon Nitride Nanoribbons: Visible-Light-Driven Photocatalytic Nitrogen Reduction, Angewandte Chemie International Edition, 58(2019) 16644-16650.

[4] H. Yu, R. Shi, Y. Zhao, T. Bian, Y. Zhao, C. Zhou, G.I.N. Waterhouse, L. Wu, C. Tung, T. Zhang, Alkali-Assisted Synthesis of Nitrogen Deficient Graphitic Carbon Nitride with Tunable Band Structures for Efficient Visible-Light-Driven Hydrogen Evolution, ADV MATER, 29(2017) 1605148.

[5] M. Humayun, W. Pi, Y. Yuan, L. Shu, J. Cao, A. Khan, Z. Zheng, Q. Fu, Y. Tian, W. Luo, A rational design of g-C_3N_4-based ternary composite for highly efficient H_2 generation and 2,4-DCP degradation, J. COLLOID INTERF. SCI., 599(2021) 484-496.

[6] M. Humayun, N. Sun, F. Raziq, X. Zhang, R. Yan, Z. Li, Y. Qu, L. Jing, Synthesis of ZnO/Bi-doped porous $LaFeO_3$ nanocomposites as highly efficient nano-photocatalysts dependent on the enhanced utilization of visible-light-excited

electrons, Appl. Catal. B-Environ., 231(2018) 23-33.

[7] Q. Hao, R. Wang, H. Lu, C.A. Xie, W. Ao, D. Chen, C. Ma, W. Yao, Y. Zhu, One-pot synthesis of C/Bi/Bi_2O_3 composite with enhanced photocatalytic activity, Appl. Catal. B-Environ., 219(2017) 63-72.

[8] K. Li, Y. Yang, A. Bacha, Y. Feng, S. Ajmal, I. Nabi, L. Zhang, Efficiently complete degradation of 2,4-DCP using sustainable photoelectrochemical reduction and sequential oxidation method, CHEM. ENG. J., 378(2019) 122191.

[9] X. Gu, J. Mei, J. Lai, S. Lv, J. Yang, S. Cui, S. Chen, Synthesis of Z-Scheme heterojunction $ZnNb_2O_6$/g-C_3N_4 nanocomposite as a high efficient photo-catalyst for the degradation of 2,4-DCP under simulated sunlight, MATER. RES. BULL., 130(2020) 110939.

[10] Y. Chen, R. Su, F. Wang, W. Zhou, B. Gao, Q. Yue, Q. Li, In-situ synthesis of CuS@carbon nanocomposites and application in enhanced photo-fenton degradation of 2,4-DCP, CHEMOSPHERE, 270(2021) 129295.

[11] Y. Chu, X. Zheng, J. Fan, Preparation of sodium and boron co-doped graphitic carbon nitride for the enhanced production of H_2O_2 via two-electron oxygen reduction and the degradation of 2,4-DCP via photocatalytic oxidation coupled with Fenton oxidation, CHEM. ENG. J., 431(2022) 134020.